

# Influence of Time-Dependent Processes on Intergranular Crack Path in 2XXX Aluminium Alloys

Gilbert Hénaff<sup>1</sup>, Frédéric Menan<sup>1</sup> et Grégory Odemer<sup>2</sup>

<sup>1</sup>Laboratoire de Mécanique et de Physique des Matériaux, UMR CNRS ENSMA Université de Poitiers 6617, ENSMA, Téléport 2, 1 avenue Clément Ader, BP 40109 86961 Futuroscope Chasseneuil, France – Email: gilbert.henaff@lmpm.ensma.fr

<sup>2</sup> Now at CIRIMAT, ENSIACET, 118 Route de Narbonne, 31077 Toulouse Cedex 04, France

**ABSTRACT.** *In this paper two examples of the influence of time-dependent processes on crack path in two 2XXX aluminium alloy are presented. The common idea is to correlate quantitative measurements of relevant fractographic features of crack path to the effects of time-dependent processes on crack growth rates. The first example is concerned with corrosion-fatigue crack growth resistance of a 2024T351 alloy cracked in the S-L direction in 3.5% NaCl solution at free corrosion potential. The crack growth enhancement induced by corrosion under certain loading conditions is accompanied by an increase in the number of smooth and flat facets on rupture surfaces which are identified as intergranular decohesions. The second example deals with the elevated temperature crack growth resistance of a 2650 T6 alloy that might be used in future supersonic aircraft fuselage panels. The creep crack growth is governed by an intergranular decohesion process induced by vacancy diffusion. The creep-fatigue crack growth at low frequency is significantly enhanced with respect to fatigue crack growth at elevated temperature. Meanwhile the intergranular fraction of the crack path is correlated with the loading period and the resulting crack growth enhancement for a fixed frequency and environment: the longer the period, the higher the crack growth enhancement and the higher the surface fraction of intergranular decohesions.*

## INTRODUCTION

The damage tolerance assessment of Aluminium Alloy (AA) structures is generally based on fatigue crack growth rates that are derived from laboratory tests that have been carried out at relatively high frequencies in order to shorten test duration. However, in many instances, time-dependent processes caused by environmental conditions such as creep or corrosion may affect crack tip deformation and damage, and as a consequence they can modify the crack growth rates as well as the crack path. Reciprocally the analysis of crack path can provide insights into the relevance of time-dependent processes during crack growth in actual components, in particular when a transition from transgranular to intergranular crack path is noticed. In this paper two examples of

such an influence of time-dependent processes on crack path in 2XXX AA are presented. First the corrosion-fatigue crack growth behaviour of a 2024-T351 AA used in many airframe components and here cracked in the S-L orientation in saline solution is examined at different frequencies. In a second part the relation between crack growth enhancement at elevated temperatures and intergranular crack path is investigated in the case of a 2650 AA that might be used in fuselage panels of next generation supersonic aircraft.

## **MATERIALS AND EXPERIMENTAL CONDITIONS**

### ***2024-T351***

The material of the study is a 2024 aluminum alloy with nominal composition Cu 4.5%, Mg 1.4%, Mn 0.60%, Fe 0.13%, Si 0.06%, Ti 0.03%, Zr+Ti 0.03%, Al balance, in the temper condition T351. The average grain size is 90  $\mu\text{m}$ , 210  $\mu\text{m}$  and 820  $\mu\text{m}$  in the short transverse S, long transverse T and laminate L direction respectively. Compact Tension specimens  $W=40$  mm, thickness  $B=10$  mm have been machined in the S-L orientation from a 50 mm thick plate provided by EADS IW. The crack plane is located at mid thickness of the plate where the highest sensitivity to intergranular corrosion is expected. Fatigue crack growth tests were conducted in the following environments: ultrahigh vacuum ( $10^{-7}$  mbar), laboratory air, distilled water, permanent immersion in a saline solution composed of distilled water with 3.5% NaCl addition ( $\text{pH} = 7$ ). Corrosion fatigue experiments were carried out under load control at free corrosion potential on a servo-hydraulic machine equipped with a specially designed Plexiglas cell. The selected value of the R load ratio was 0.7 in order to avoid crack closure effects [1]. More details can be found elsewhere [1-3].

### ***2650 T6***

The 2650 alloy is a copper-magnesium aluminium alloy, provided in the form of sheets by Rhénalu (thickness: 2.5 and 5mm). The Fatigue Crack Growth (FCG) and Creep Fatigue Crack Growth (CFCG) resistance of this alloy was investigated after T6 artificial ageing treatment ( $192^{\circ}\text{C}$  for 21 hours) resulting into a fully recrystallised microstructure with an average grain size of  $40\mu\text{m}$  in the rolling plane. CCG, FCG and CFCG testing were performed on CT specimens ( $W=32\text{mm}$ ) of 5 mm thickness in the L-T orientation. FCG and CFCG were conducted on a servohydraulic machine equipped with a furnace, using a constant load ratio  $R=0.5$ . Additional information are available in [4-7].

## **RESULTS AND ANALYSIS**

### ***Corrosion-Fatigue Crack Growth in 2024 T351 in the S-L direction***

The corrosion-fatigue crack growth rates in saline solution were measured at different frequencies in order to investigate the effect of time-dependent processes. The results are reported in Figure 1a. Almost surprisingly a FCG enhancement is observed at high

frequencies [2.5-10Hz], while Fatigue Crack Growth Rates (FCGRs) measured at 0.1 Hz are comparable to those observed in air or in distilled water despite of the longer exposure duration to the corrosive medium. Nevertheless it is noteworthy that these two environments in turn induce a significant FCGR enhancement with respect to ultra-high vacuum. More precisely, it has been shown that the enhancement observed in saline solution is governed by the rise time RT [3], as shown in Figure 1b. Characteristic FCG regimes in saline solution have thus been identified; they are schematically presented in Figure 3. The corrosion-assisted regime controlled by short RT is characterised by a 2<sup>nd</sup> power-law exponent, while the behaviour observed at longer RT values as well as in air or distilled water can be accounted for by a 4<sup>th</sup> power law.

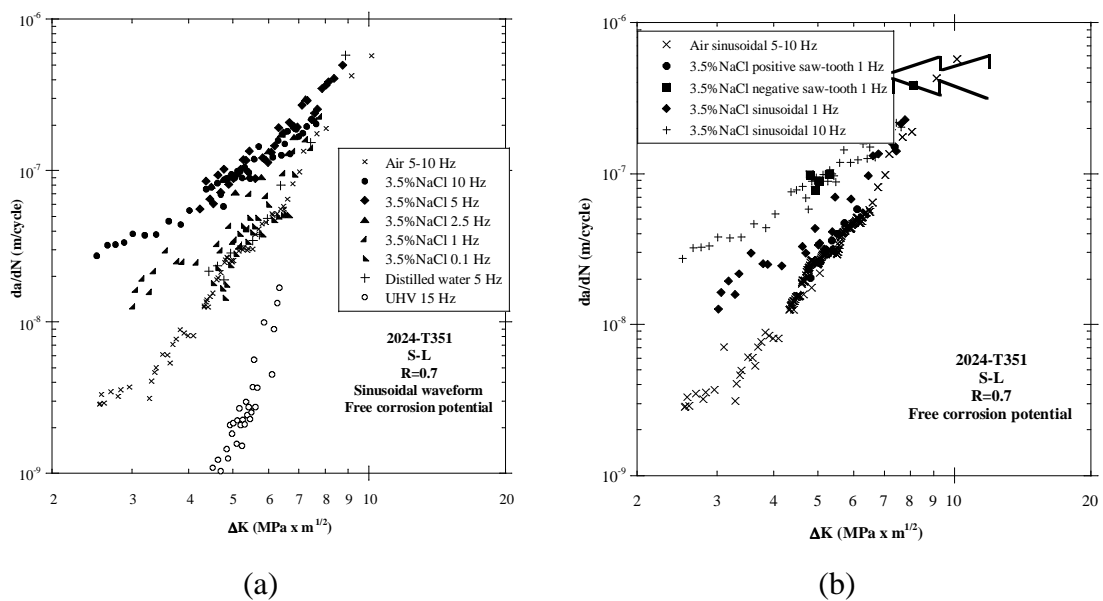


Figure 1. Corrosion fatigue crack growth rates measured as a function of  $\Delta K$  (a) at different frequencies in saline solution in comparison with high vacuum, air and distilled water; (b) under different loading waveforms in saline solution.

These measurements are actually consistent with crack path observations. Indeed fracture surfaces produced in vacuum are typical of the crystallographic stage I-like cracking mode (Figure 2a), which is common for cracking of 2XXX aluminum alloys in inert environment [8, 9]. Meanwhile fracture surfaces produced in air, distilled water and in saline solution at different frequencies, may look similar at a first glance, with a transgranular, cleavage-like cracking mode (Figure 2b-c-d) and the formation of dimples around coarse intermetallic particles, especially for high  $\Delta K$  values. However, at lower  $\Delta K$  values in saline solution, i. E. in conditions where the corrosion-assisted FCG mechanism is observed, the presence of some flat, large and smooth facets on fracture surfaces is noticed. These facets are pointed out by the small dark arrows in

Figure 2 (f). While the presence of such facets is also noticed in air, they are more numerous and larger (Figure 2 (e) and (f)) in saline solution.

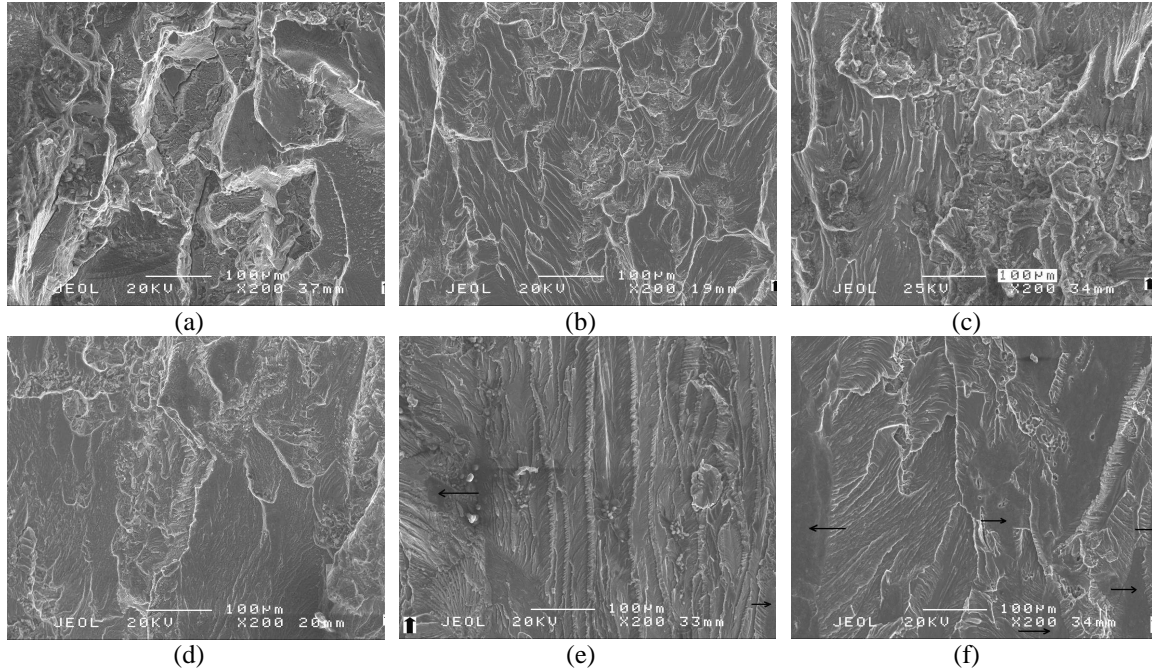


Figure 2. Fatigue fracture surfaces produced at  $\Delta K=6 \text{ MPa}\sqrt{\text{m}}$  under sinusoidal waveform; (a) ultra high vacuum 15 Hz; (b) air 5-10 Hz (c) distilled water 5 Hz; (d) 3.5% NaCl solution 10 Hz;  $\Delta K=3 \text{ MPa}\sqrt{\text{m}}$ , 10 Hz, (e) air (f) 3.5% NaCl (crack propagation from bottom to top).

In order to establish a possible relation between the activation of this corrosion-assisted regime and the presence of such facets, quantitative measurements of the fracture surface occupied by those facets have been performed. These data have been reported on a  $da/dN-\Delta K$  graph in Figure 4. The percentages of facets in 3.5% NaCl at 1 Hz with a sinusoidal waveform indicate that in the regime where the Paris law exponent is approximately equal to 4, the increase in the FCGRs can also be correlated with the increase in the area of facets. Indeed, at  $\Delta K=4 \text{ MPa}\sqrt{\text{m}}$  in air the facets represent 2% of the total area, whereas in 3.5% NaCl at 1 Hz with a sinusoidal waveform the formation of these facets is promoted since they occupy 18% of the total surface area. In order to identify the nature of the flat, large and smooth facets, etch pitting of the fracture surfaces has been realized. In 3.5% NaCl solution, the shape of the facets is neither square (typical of near  $\{100\}$  crystallographic plane) nor triangle (typical of near  $\{111\}$  crystallographic plane). These pits may correspond to higher index planes not associated with a grain boundary. However, it should be noticed that different pit shapes are observed over a single facet (Figure 5), which does not support such an assumption. In addition the similarity in the morphology of these facets with the shape and the size of the grains suggest that they correspond with a locally intergranular crack path.

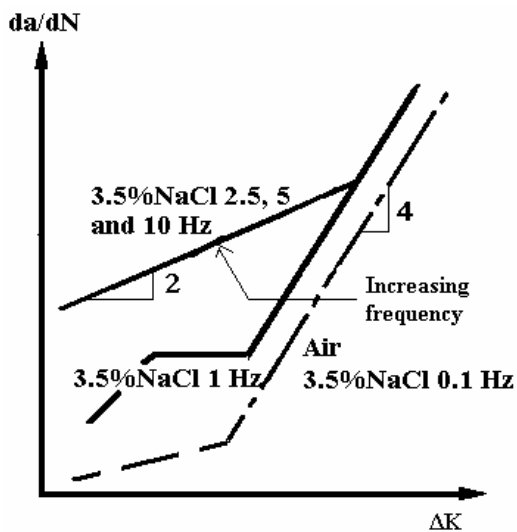


Figure 3. Influence of the loading frequency on the FCGRs of the alloy 2024-T351 for a sinusoidal waveform (R=0.7, S-L orientation).

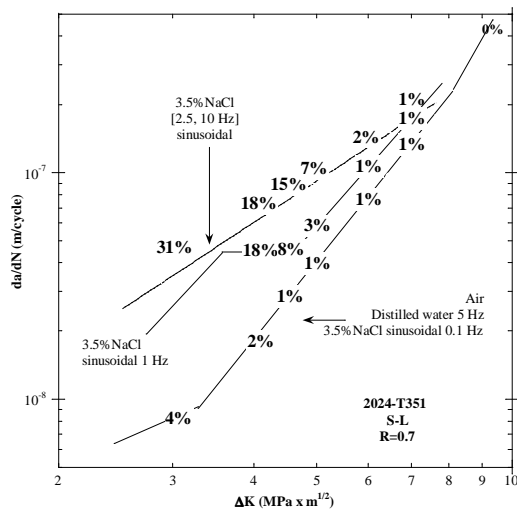


Figure 4. Percentages of flat facets for the S-L orientation plotted on a da/dN-ΔK graph.

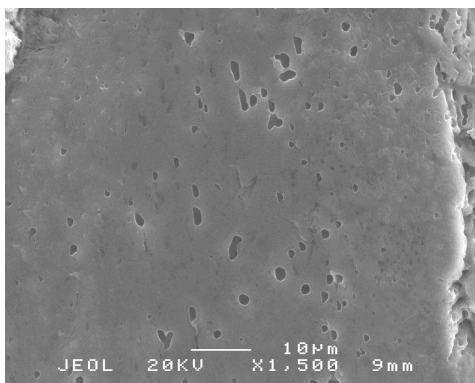


Figure 5. Identification of the flat, large and smooth facets in air and saline solution by Keller's reagent etch pitting (R=0.7, 5 Hz, sinusoidal waveform, 3.5% NaCl,  $\Delta K=5.7 \text{ MPa}\sqrt{\text{m}}$ ).

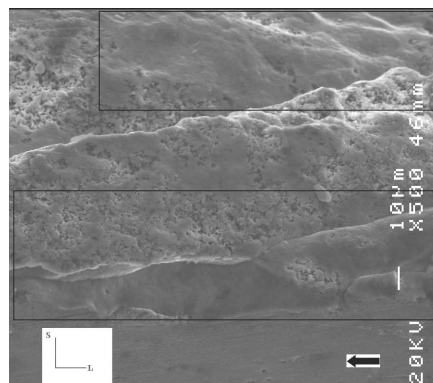


Figure 6. Morphology of the facets in saline solution. 2024-T351 S-L. R=0.7. 10 Hz.  $\Delta K=4-4.5 \text{ MPa}\sqrt{\text{m}}$ . Black arrow : crack propagation direction.

Finally it is noteworthy that in the T851 in the S-L orientation temper or the L-T orientation in the T351 temper the facets are much less numerous, while these conditions corresponds with a much higher resistance to intergranular stress corrosion cracking [1], which provides an additional support for the intergranular nature of these facets and for a relation between the SCC susceptibility of 2XXX aluminum alloys and a pronounced FCG enhancement in saline solution determined by the

orientation between the load direction and the grain orientation on one hand and the presence of a continuous anodic network along the grain boundaries determined by aging conditions on the other hand.

### ***Creep fatigue crack growth in 2650 alloy***

The CFCG rates measured under trapezoidal load signal with different hold time duration are presented for a test temperature of 130°C and in Figure 7b for 175°C. It can be seen that the introduction of hold time induces a significant crack growth enhancement and that this enhancement is more pronounced as the test temperature is raised. This behaviour is indicative of a possible additional damage mechanism induced by creep. Fracture surface observations are therefore expected to provide further insights into this issue. Indeed the creep crack growth resistance was previously examined [5] and it was shown that CCG fracture surfaces exhibit two characteristic failure modes: an intergranular fracture mode prevailing in the slow growth rate regime (Figure 8 a) and a mixture of intergranular and ductile fractures before failure. The intergranular cracking mode in AA occurs by cavitation controlled by vacancy diffusion along grain boundaries [10, 11]. Indeed CFCG fracture surfaces also exhibit significant amounts of intergranular decohesions. Quantitative measurements of area fraction occupied by intergranular facets at 130°C and 175°C are presented in Figure 9 a and Figure 9 b, respectively. It can be noticed that the longer the hold time, the higher the amount of intergranular facets, especially at low K values. Nevertheless, even for hold times as high as 3000s, the amount of intergranular facets is lower than during CCG at the same K or  $K_{max}$  value for a fixed temperature. For a given hold time value, the percentage of intergranular facets is higher at 175°C than at 130°C. Additional results have shown that this relation between CFCG enhancement and the promoted formation of intergranular facets still holds in UHV, and that for a given loading condition the amount of IF is higher in vacuum than in air [4-7].

## **CONCLUSIONS**

This paper has presented evidences that an intergranular crack path can be produced under cyclic loading in 2XXX AA under conditions where time-dependent processes such as corrosion or creep affect the damage process at the crack tip. As regards corrosion fatigue in 2024 T351 alloy in the S-L, it has been shown that a significant fraction of fracture surfaces are occupied by intergranular facets when a corrosion-assisted crack growth mechanism, controlled by load rise time, is activated. A relation between stress corrosion cracking sensitivity and corrosion-assisted crack growth mechanism can thus be established. Besides intergranular decohesions are observed both during creep crack growth and fatigue crack growth at low frequencies and elevated temperatures in the 2618 alloy. More precisely, the amount of intergranular

facets can be related to the load period and as a consequence to the crack growth enhancement during cyclic loading at low frequencies for a given environment.

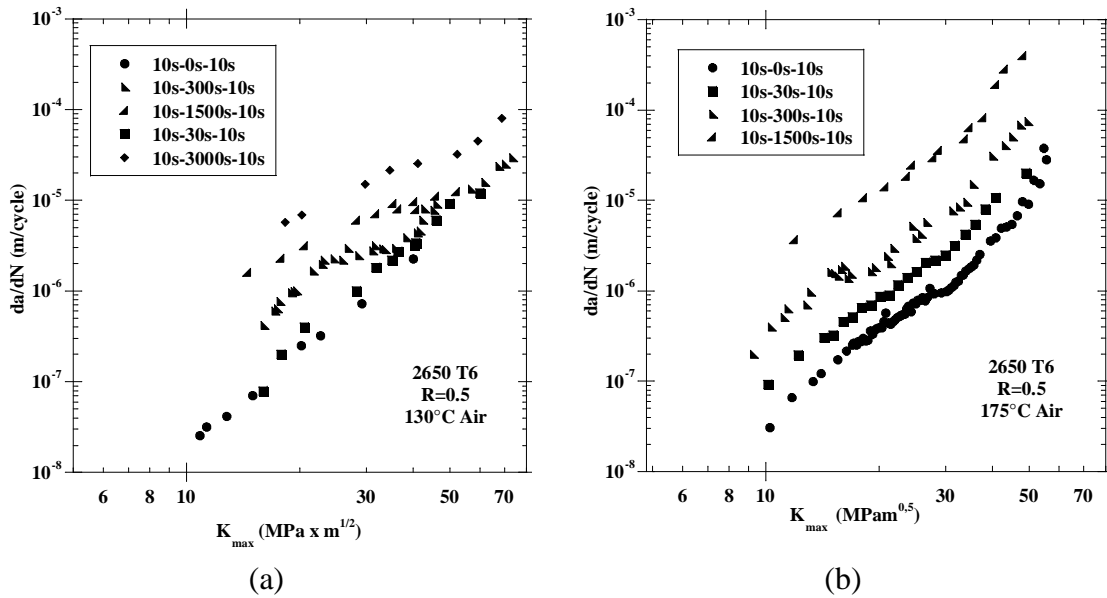


Figure 7: Influence of hold time on creep-fatigue crack growth rates at R=0.5 (a) at 130°C; (b) at 175°C.

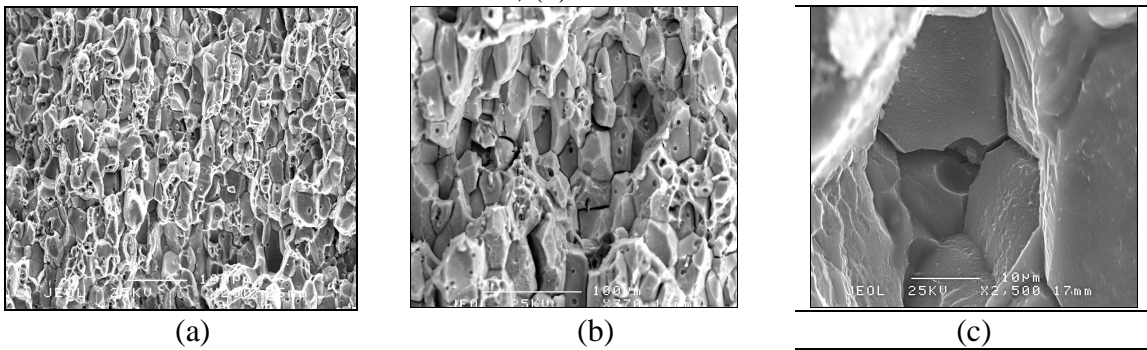


Figure 8: fracture surfaces produced during (a) CCG ( $K=22 \text{ MPa} \times \text{m}^{1/2}$ , 175°C), (b) CFCG ( $K_{\max}=23 \text{ MPa} \times \text{m}^{1/2}$ ,  $da/dN = 2 \times 10^{-5} \text{ m/cycle}$ , 10s-1500s-10s, 175°C) (c) cavitation at triple grain boundary ( $K_{\max}=30 \text{ MPa} \times \text{m}^{1/2}$ ,  $da/dN = 2 \times 10^{-6} \text{ m/cycle}$ , 10s-300s-10s, 175°C).

## REFERENCES

1. Menan, F. and Henaff, G. (2009) *International Journal of Fatigue* in press.
2. Menan, F. (2008) *Influence de la Corrosion Saline sur la Tolérance aux Dommages d'un Alliage d'Aluminium Aéronautique 2XXX*, PhD thesis, University of Poitiers, France: Futuroscope Chasseneuil.

3. Menan, F. and Henaff, G. (2009) *Materials Science & Engineering A* to be published.
4. Odemer, G., Benoit, G., Koffi, E., Hénaff, G., and Journet, B. (2009) *International Journal of Fatigue* **in press**.
5. Odemer, G., Henaff, G., and Journet, B. (2006) *Scripta Materialia* **54**(1), 51-55.
6. Henaff, G., Odemer, G., and Tonneau-Morel, A. (2007) *International Journal of Fatigue* **29**(9-11), 1927-1940.
7. Odemer, G., Hénaff, G., Journet, B., and Rémy, L. (2006). in *Fatigue'2006, 9th International Congress on Fatigue*, S. Johnson, D.L. McDowell, J.C. Newman Jr, and A. Saxena, (Ed), Elsevier: Atlanta, Georgia, USA.
8. Petit, J., Hénaff, G., and Sarrazin-Baudoux, C. (2003). In *Comprehensive Structural Integrity*, pp. 211-280, J. Petit and P. Scott, (Eds), I. Milne, R.O. Ritchie, and B. Karihaloo Eds, Elsevier.
9. Ro, Y., Agnew, S.R., and Gangloff, R.P. (2007) *Metallurgical and Materials Transactions a-Physical Metallurgy and Materials Science* **38A**(12), 3042-3062.
10. Yang, L. (1995) *Metallurgical and materials transactions A Physical metallurgy and materials science* **26**(2), 315-328.
11. Vitek, V. (1978) *Acta Metallurgica* **26**(9), 1345-1356.
12. Odemer, G. (2005) *Tolérance au dommage avec prise en compte des interactions fatigue-fluage de l'alliage 2650-T6*, PhD thesis, ENSMA, Poitiers.

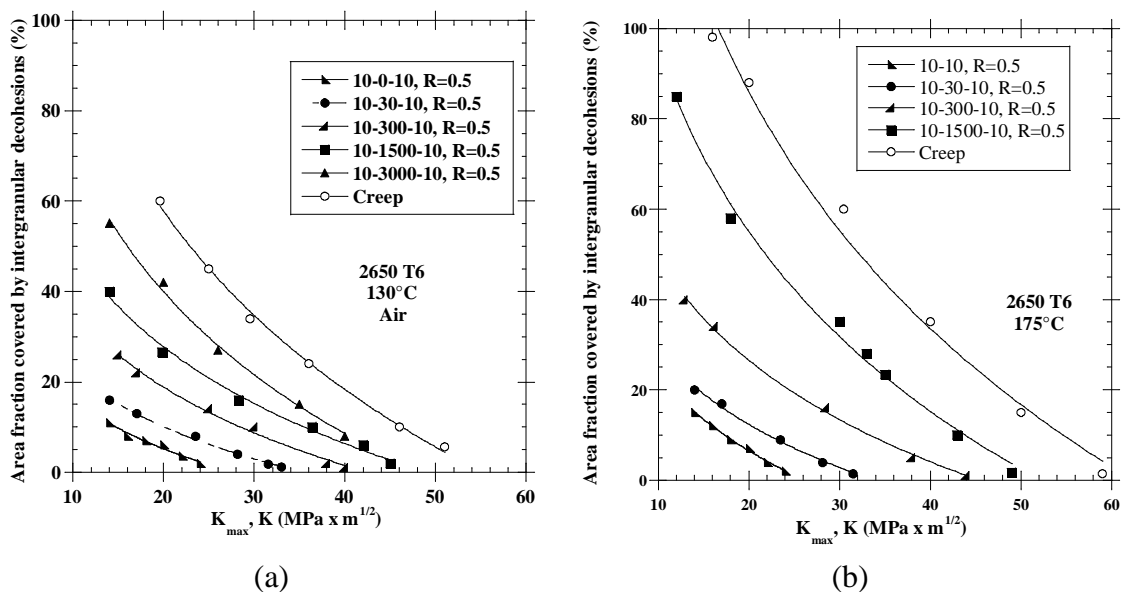


Figure 9: Percentage of area covered by intergranular decohesions as a function of maximum stress intensity factor for different loading cases (a) at 130°C; (b) at 175°C.